Isentropes of spin-1 bosons in an optical lattice

K. W. Mahmud,[1] G. G. Batrouni,[2] and R. T. Scalettar[1]
[1]*Physics Department, University of California, Davis, California 95616, USA*
[2]*INLN, Université de Nice-Sophia Antipolis, CNRS; 1361 route des Lucioles, F-06560 Valbonne, France*
(Received 6 October 2009; published 17 March 2010)

We analyze the effects of adiabatic ramping of optical lattices on the temperature of spin-1 bosons in a homogeneous lattice. Using mean-field theory, we present the isentropes in the temperature-interaction strength (T, U_0) plane for ferromagnetic, antiferromagnetic, and zero spin couplings. Following the isentropic lines, temperature changes can be determined during adiabatic loading of current experiments. We show that the heating-cooling separatrix lies on the superfluid-Mott phase boundary with cooling occurring within the superfluid and heating in the Mott insulator and quantify the effects of spin coupling on the heating rate. We find that the mean-field isentropes for low initial entropy terminate at the superfluid–Mott-insulator phase boundary.

DOI: 10.1103/PhysRevA.81.033609 PACS number(s): 03.75.Hh, 03.75.Mn, 05.30.Jp, 75.10.Jm

I. INTRODUCTION

Ultracold atoms in optical lattices offer the possibility of realizing various fundamental models of strongly correlated bosons and fermions [1,2]. A crucial aspect of the optical lattice system is its flexibility in controlling different lattice parameters and particle interactions, thereby facilitating progress toward the creation of quantum emulators. After the observation of the superfluid to Mott insulator transition with spin-0 bosons [1], steady progress has been made toward trapping spinful atoms. These models, along with a precise knowledge and tunability of the microscopic Hamiltonian can potentially lead to a better understanding of quantum magnetism and related phenomena. Unlike magnetic traps, which freeze the F_z component of spin, optical traps can confine ^{23}Na, ^{39}K, and ^{87}Rb with hyperfine spin $F = 1$. Several theoretical studies focused on spinor condensates in an optical lattice [3–7] and how the spin degree of freedom modifies the phase diagram and the nature of superfluid–Mott-insulator transition. Experiments also explored the properties of spinful bosons in harmonic traps [8], and recently, in a double well optical superlattice [9].

The technological breakthrough in cooling to ultracold temperatures paved the way for the realization of Bose-Einstein condensation and optical lattice experiments. The temperature of a bosonic gas in a trap can be measured accurately. However, no established temperature measurement exists for optical lattice systems, although several proposals were made [10,11]. This makes it difficult to obtain a quantitative description of the various low temperature phases and thermal and quantum phase transitions between them [12].

In current experiments, ultracold atoms are first loaded in a harmonic trap and then an external sinusoidal potential created by interfering lasers are slowly ramped up to create the optical lattice. For gradual enough ramping, there is no heat exchange with the environment and this process can be considered adiabatic (constant entropy) [1,13]. It is of great interest to the experimentalists to know how the system cools down or heats up during the adiabatic process. The change in temperature with adiabatic ramp-up of optical lattice for the spinless Bose-Hubbard model and the Fermi Hubbard model was studied by several authors [14–18].

In this article, we present the isentropes for spin-1 bosons in a homogeneous optical lattice for both ferromagnetic and antiferromagnetic spin couplings. We investigate the effects of adiabatic ramping on temperature within the mean-field approximation and show that for spinor bosons cooling occurs in the superfluid phase and heating occurs in the Mott insulator or normal phase. We find that the heating-cooling separatrix lies along the superfluid-Mott phase boundary. As the magnitude of spin coupling increases, the rate of temperature change decreases in the Mott regime and can both increase and decrease in the superfluid regime depending on the value of the spin coupling. We find that the mean-field isentropes for low initial entropy terminate at the superfluid–Mott-insulator phase boundary and argue that this is a consequence of the absence of breaking of the degeneracy of the ground state in the mean-field approximation.

The article is organized as follows. We discuss the spin-1 Bose-Hubbard model and the details of the mean-field theory in Sec. II. In Sec. III, we investigate the entropy for this model and present our results for the isentropes and temperature changes for different couplings. A summary is contained in Sec. IV.

II. SPIN-1 BOSE-HUBBARD MODEL AND MEAN-FIELD THEORY

The Hamiltonian for spin-1 bosons in an optical lattice is given by

$$H = -t \sum_{\langle i,j\rangle,\sigma} (a^\dagger_{i\sigma} a_{j\sigma} + a^\dagger_{j\sigma} a_{i\sigma}) + \frac{U_o}{2} \sum_i \hat{n}_i(\hat{n}_i - 1) + \frac{U_2}{2} \sum_i \left(\vec{F}_i^2 - 2\hat{n}_i\right) - \sum_i \mu_i \hat{n}_i. \quad (1)$$

Here $a^\dagger_{i\sigma}$ ($a_{i\sigma}$) are boson creation (destruction) operators at site i with spin component σ ($\sigma = 1, 0, -1$). The first term in Eq. (1) describes the spin-dependent hopping between near-neighboring sites. In the second term, U_o is the on-site repulsion and $\hat{n}_i = \sum_\sigma a^\dagger_{i\sigma} a_{i\sigma}$ counts the total number of bosons on site i. In the third term, U_2 is the spin-dependent interaction, which can be zero, positive, or negative, and $\vec{F}_i = \sum_{\sigma,\sigma'} a^\dagger_{i\sigma} \vec{F}_{\sigma\sigma'} a_{i\sigma'}$ is the total spin on site i, where $\vec{F}_{\sigma\sigma'}$ are the standard spin-1 matrices.

The spin-dependent interaction U_2 for the spin-1 model greatly modifies its physics compared to that of spin-0

bosons [7]. From the symmetry of the bosonic wave function, scattering with total spin $F = 1$ is prohibited. The difference in scattering lengths in the $F = 0$ (a_0) and $F = 2$ (a_2) channels is responsible for the spin-dependent coupling. The interactions can be expressed as $U_0 = 4\pi\hbar^2(a_0 + 2a_2)/3M$ and $U_2 = 4\pi\hbar^2(a_2 - a_0)/3M$, M being the mass of the atom. The spin-dependent interaction is ferromagnetic when $U_2 < 0$ ($a_2 < a_0$) and antiferromagnetic when $U_2 > 0$ ($a_2 > a_0$). ^{23}Na atoms are ferromagnetic and ^{87}Rb antiferromagnetic. Our study in this article considers both signs of the interaction. The coupling constants obey the constraint $-1 < U_2/U_0 < 1/2$.

The zero-temperature phase diagram for the spin-1 model was calculated with numerical methods such as quantum Monte Carlo (QMC) [6,19], density-matrix renormalization group (DMRG) [20], and also within the mean-field approximation [7,21]. As for the spin-0 case, mean-field theory for the spin-1 Bose-Hubbard model [7,22,23] captures the essential physics of this system. A finite temperature extension of the mean-field analysis was presented in Ref. [7], revealing the rich phase diagram that includes both first and second-order transitions. The spinor Bose-Hubbard model, with filling of one boson per site and for small hopping, can be mapped onto the $F = 1$ bilinear biquadratic Heisenberg model, which was studied by many authors [24–26] to gain an understanding of different Mott phases. Here, we will extend the mean-field calculation presented in Ref. [7] to obtain the entropy.

In the mean-field approximation, the hopping term is decoupled as

$$a^\dagger_{i\sigma} a_{j\sigma} \simeq \langle a^\dagger_{i\sigma}\rangle a_{j\sigma} + a^\dagger_{i\sigma}\langle a_{j\sigma}\rangle - \langle a^\dagger_{i\sigma}\rangle\langle a_{j\sigma}\rangle, \tag{2}$$

neglecting fluctuations around the equilibrium value. Here, we define $\psi_\sigma = \langle a^\dagger_{j\sigma}\rangle = \langle a_{j\sigma}\rangle$, for $\sigma = 1, 0, -1$ to be the superfluid order parameter. The use of Eq. (2) allows us to rewrite Eq. (1) as a sum of independent single-site Hamiltonians, $H = \sum_i H_i^{\mathrm{mf}}$ where

$$H_i^{\mathrm{mf}} = \frac{U_o}{2}\hat{n}_i(\hat{n}_i - 1) + \frac{U_2}{2}\left(\vec{F}_i^2 - 2\hat{n}_i\right) - \mu\hat{n}_i - \sum_\sigma \psi_\sigma(a^\dagger_{i\sigma} + a_{i\sigma}) + \sum_\sigma |\psi_\sigma|^2. \tag{3}$$

Here we set $zt = 1$, where z is the number of nearest neighbors. To perform the mean-field calculations, we write the matrix elements of the Hamiltonian H_i^{mf} in the occupation number basis $|n_{i,-1}, n_{i,0}, n_{i,1}\rangle$ and truncate the on-site Hilbert space H_i by allowing a maximum number of particles per site, $\mathrm{N_{max}} = 4$, for which the truncation effects are negligible. We use $\mathrm{N_{max}} = 6$ for simulations with higher number density such as in Fig. 7. Since we are treating a homogeneous system, the site index i can be ignored. We diagonalize the Hamiltonian to obtain the energy spectrum E_α and eigenstates $|\phi_\alpha\rangle$ and evaluate the partition function and the free energy,

$$Z(\mu, U_0, U_2, T; \psi_\sigma) = \sum_\alpha e^{-E_\alpha/T}, \tag{4}$$

and

$$\mathcal{F}(\mu, U_0, U_2, T; \psi_\sigma) = -T \ln Z(\mu, U_0, U_2, T; \psi_\sigma). \tag{5}$$

We set $k_B = 1$ throughout our calculation. For given μ, U_0, U_2, and T, the superfluid order parameters ψ_σ are obtained by minimizing the free energy (i.e., by solving $\partial\mathcal{F}/\partial\psi_\sigma = 0$ for $\sigma = 1, 0, -1$). Solving for the extrema of the free energy is equivalent to the self-consistency condition for ψ_σ.

After determining the values of the superfluid order parameters ψ_{-1}^{eq}, ψ_0^{eq}, and ψ_1^{eq} that minimize the free energy, other physical quantities can be obtained easily from the resulting global minimum of free energy $\mathcal{F}^{\mathrm{eq}}$, and eigenvalues ($E_\alpha^{\mathrm{eq}}$) and eigenstates ($\phi_\alpha^{\mathrm{eq}}$) at the global minimum. The superfluid density is given by

$$\rho_S = \sum_\sigma \left|\psi_\sigma^{\mathrm{eq}}\right|^2, \tag{6}$$

and the number density is

$$\rho = -\partial\mathcal{F}/\partial\mu = \frac{1}{Z}\sum_\alpha e^{-E_\alpha^{\mathrm{eq}}/T}\left\langle\phi_\alpha^{\mathrm{eq}}\middle|\hat{n}\middle|\phi_\alpha^{\mathrm{eq}}\right\rangle. \tag{7}$$

Finally, the entropy is calculated from

$$S = -\partial\mathcal{F}/\partial T = \ln Z + \frac{1}{ZT}\sum_\alpha E_\alpha^{\mathrm{eq}} e^{-E_\alpha^{\mathrm{eq}}/T}. \tag{8}$$

Pai *et al.* [7] gave a detailed analysis of the superfluid order parameters $\psi_1, \psi_0, \psi_{-1}$ for different phases and showed that, in the antiferromagnetic (polar) superfluid, the possibilities are $\psi_1 = \psi_{-1} > 0$, $\psi_0 = 0$, and $\psi_1 = \psi_{-1} = 0$, $\psi_0 > 0$. For the ferromagnetic superfluid, $\psi_1 = \psi_{-1}$, $\psi_0 = \sqrt{2}\psi_1$.

We use the superfluid density to determine the phase diagram in the (T, U_0) plane. $\rho_s > 0$ corresponds to the ferromagnetic or polar superfluid and $\rho_s = 0$ corresponds to the Mott-insulator phase. At finite temperature, there is a crossover from the Mott phase to the normal phase depending on the value of the compressibility.

III. ENTROPY AND ISENTROPIC CURVES

Figure 1(a) shows the entropy (S) and density (ρ) at zero temperature for $U_2 = 0$, $U_0 = 12zt$ (we set the energy scale $zt = 1$ throughout our calculation) for an increasing chemical potential along a vertical cross section in the (μ, U_0) phase diagram. This trajectory traverses the superfluid regions with noninteger ρ as well as Mott plateaux with density fixed at integral values $\rho = 1$ and 2. We observe that at $T = 0$, although the entropy (S) is zero in the superfluid (SF) region, it is nonzero in the Mott insulator (MI) lobes. For $\rho = 1$, the entropy is ln(3) and for $\rho = 2$ the entropy $S = \ln(6)$. This nonzero ground-state entropy can be understood as follows. In the mean-field treatment, the system Hamiltonian is a sum of single-site Hamiltonians and in the MI phase for one particle per site, three degenerate spin components $\sigma = -1, 0, 1$, contribute to $S = \ln(3)$. For the $\rho = 2$ Mott phase, the two spin-1 bosons on a single site have total spin $F = 0, 2$, with $F = 1$ eliminated by the symmetry constraint on the spin functions. The number of degenerate components is therefore 5 due to $F = 2$, and 1 due to the spin singlet $F = 0$, so that $S = \ln(6)$.

The entropy for the ferromagnetic case $U_2 < 0$, $U_2 = -0.1U_0$, $U_0 = 12$ at $T = 0$ is shown in Fig. 1(b). A negative value of the spin coupling U_2 favors maximal total spin. Hence, $F = 2$ for $\rho = 2$, and $S = \ln(5)$ is reduced from its $U_0 = 0$ value. For $\rho = 1$ (i.e., the first Mott lobe) the entropy is still ln(3) as before and zero in the superfluid regime.

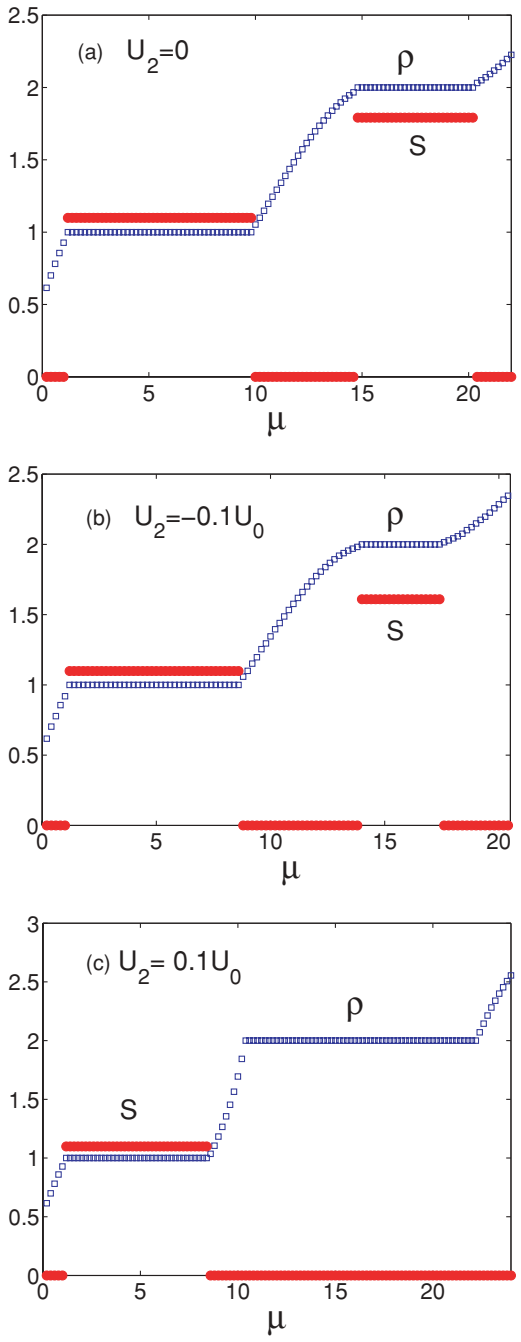

FIG. 1. (Color online) Entropy and filling as functions of chemical potential at zero temperature for $U_0 = 12zt$ (we set $zt = 1$ in our calculation) and (a) $U_2 = 0$, (b) $U_2 = -0.1U_0$, and (c) $U_2 = 0.1U_0$. For $U_2 = 0$, the entropy is ln(3) at $\rho = 1$, ln(6) at $\rho = 2$, and zero elsewhere. This can be understood in terms of the degeneracy of spin-1 (three component) bosons and total spin at each site. For $U_2 < 0$, the energy is minimized with maximum total spin $F = 2$ and hence the entropy at $\rho = 2$ changes to ln(5). Similarly, for $U_2 > 0$, the ground state has lowest total spin $F = 0$, and hence the system has zero entropy for $\rho = 2$.

Antiferromagnetic values, $U_2 > 0$, favor the $F = 0$ singlet phase for $\rho = 2$ and therefore $S = 0$ for the second Mott lobe. Figure 1(c) shows the entropy for $U_2 = 0.1U_0$, $U_0 = 12$ at $T = 0$. As in the earlier cases, the entropy is zero in the SF

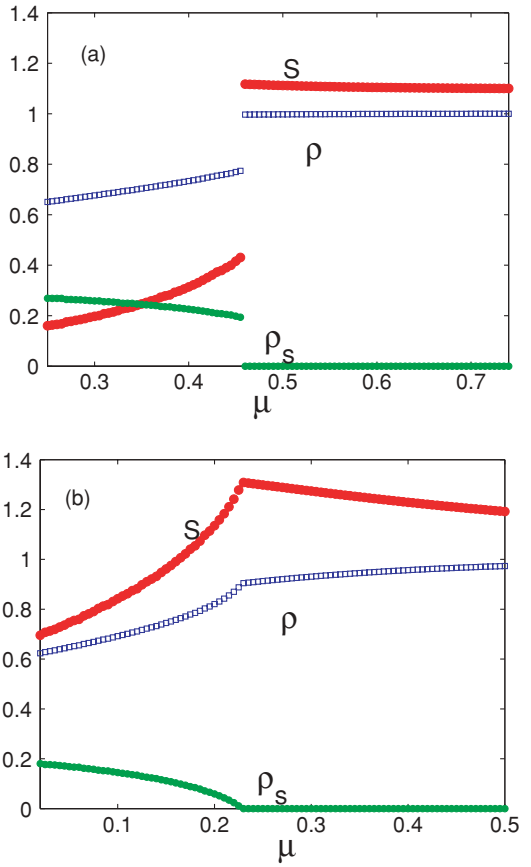

FIG. 2. (Color online) Traversing a (a) first-order and (b) second-order phase boundary in the (μ, T) plane. (a) $T = 0.1$ and (b) $T = 0.2$. The discontinuity in the entropy in (a) satisfies the Clausius-Clapeyron equation relating the entropy jump to the slope of the first-order phase boundary. Here $U_0 = 12$, $U_2 = 0$.

phase and ln(3) in the first MI lobe. The presence of finite entropy for the MI phase in mean-field theory even at $T = 0$, influences the topology of the isentropic curves, as we shall discuss.

In contrast to spin-0 bosons, spin-1 bosons in a lattice exhibit both first and second-order phase transitions at finite temperature. Here we examine the entropy across these different phase boundaries. In Fig. 2(a), discontinuities in entropy, density, and superfluid density are evident across a first-order phase boundary in the (μ, T) plane at a constant $T = 0.1$ and $U_0 = 12$, $U_2 = 0$. Such first-order finite temperature phase transitions should follow the Clausius-Clapeyron equation from thermodynamics, which relates the discontinuity in the entropy and other parameters to the slope of the phase boundary. We verified that our results indeed satisfy this identity. For example, in Fig. 2(a), we find $\Delta S/\Delta\rho = 3.10$, which equals the slope $d\mu/dT$ in the (μ, T) plane.

As we increase the temperature, the entropy jump decreases and finally vanishes at the tricritical point. The entropy is continuous afterward across a second-order phase transition as we show in Fig. 2(b) for $T = 0.2$.

To investigate further the effect of adiabatic ramping of the optical lattice, we calculate the entropy at different couplings (fixed U_2 and many U_0) and temperatures, and construct the isentropic curves in the (T, U_0) plane. Figure 3(a) shows the

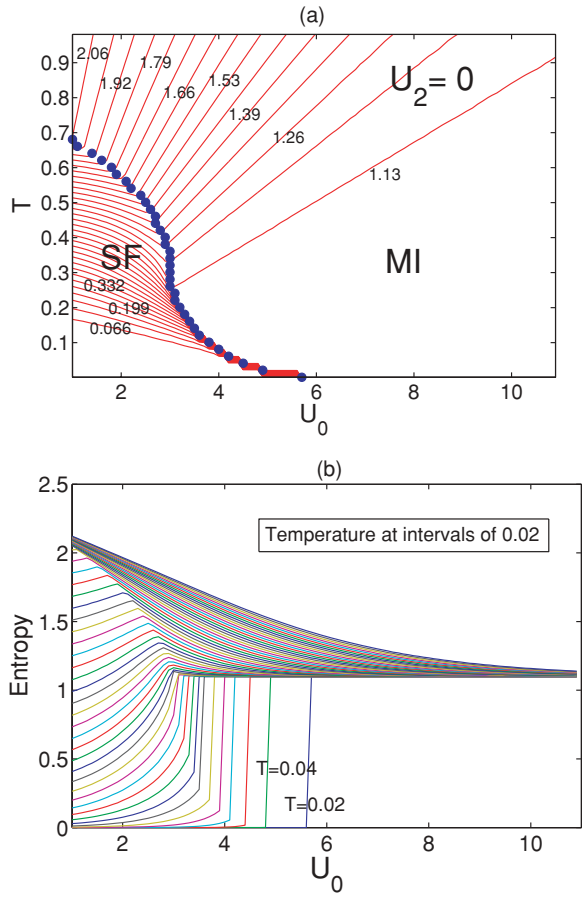

FIG. 3. (Color online) (a) Isentropic curves overlaid on the finite temperature phase diagram for $U_2 = 0$ and density $\rho = 1$. During adiabatic ramping of the lattice, the system cools along the isentropic lines in the superfluid region and heats in the Mott region. In our mean-field analysis, the separatrix of cooling and heating lies on the superfluid-Mott phase boundary in the (T, U_0) plane. (b) Shows entropy as a function of U_0 at constant temperatures for intervals of $T = 0.02$. The termination of the isentropic lines at the phase boundary can be understood by the absence of low entropy states as U_0 increases into the Mott regime.

isentropic curves for $U_2 = 0$ for fixed occupation number $\rho = 1$. Isentropic curves are overlaid on the finite temperature phase diagram where the boundary separates $\rho_s > 0$ (SF phase) and $\rho_s = 0$ (MI or Normal phase). During adiabatic ramping of the lattice, the system heats or cools following one of these isentropic lines. For entropy 1.13 at $U_0 = 0$ the temperature starts at $T = 0.43$ but decreases along the isentrope as U_0 rises. At the SF boundary, T begins to rise again. In fact, all the mean-field isentropes that we obtain show this pattern—there is cooling in the SF regime and heating in the MI regime with the heating-cooling separatrix exactly on the phase boundary.

The occurrence of cooling in the SF phase and heating in the Mott phase, and the location of the heating-cooling separatrix exactly on the phase boundary can be understood with the following physical argument—moving away from the phase boundary toward higher U_0, one enters the Mott phase with reduced number fluctuations and an integer number of atoms per site. So, as U_0 increases at constant T, the entropy is reduced. Therefore, if we want to keep the entropy constant as U_0 increases, the temperature must rise, and there is heating in the Mott phase. Similarly, moving away from the phase boundary toward the SF regime by decreasing U_0, more and more particles enter the condensate, reducing the quantum depletion. More particles entering the condensate means entropy is decreasing since the condensate carries no entropy. So, to keep S constant as U_0 decreases in the SF, there must again be heating in the system.

The fact that within mean-field theory phase boundaries also demark the switch between cooling and heating isentropes is a phenomenon that was also observed in studies of classical models of nuclear magnetism [27]. Recently, it was also shown that the spin-1 Blume-Capel model exhibits this same behavior [28]. In both cases, it is found that in exact Monte Carlo calculations for the same models the heating-cooling separatrix continues to track the phase boundary qualitatively, but increasingly breaks away as the temperature increases.

Another feature of the isentropic lines is that for low initial entropy (which is also at low temperature) they terminate at the SF-MI phase boundary without ever entering the MI phase. Figure 1 showed that, within site-decoupled mean-field theory, the entropy in the Mott regime with $\rho = 1$ is $\ln(3) = 1.0986$ even at $T = 0$. As a consequence, if we follow an isentrope with initial entropy less than $\ln(3)$ in the SF phase, as U_0 increases beyond the critical value, the isentrope cannot reach the MI phase because of its high ground-state spin entropy.

Figure 3(b) shows entropy as a function of U_0 at constant temperature intervals. As U_0 increases into the MI at constant temperature, the low entropy values go to $S \geqslant 1.0986$. This illustrates why only the isentropes with $S > 1.0986$ in Fig. 3(a) continue to the MI phase. This termination of the isentropic lines is a shortcoming of the mean-field theory treatment. There has not been any exact numerical study of isentropic lines for the spin-1 model within QMC or DMRG.

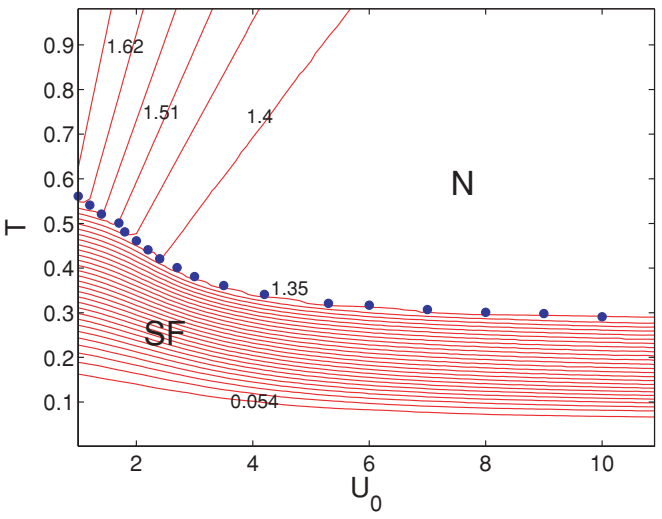

FIG. 4. (Color online) Isentropic curves for a noninteger filling, $\rho = 0.7$ and $U_2 = 0$. As in the commensurate filling case, the heating-cooling separatrix lies on the phase boundary. However, the low temperature isentropes do not terminate and remain under the phase boundary.

In the Mott phase with independent sites, any of the three choices $\sigma = 0, \pm 1$ is possible on each site. However, it is clear that this degeneracy is broken in perturbation theory in t. Two adjacent sites with the same σ will have a second-order lowering $\Delta E^{(2)} = -8t^2/U$ while adjacent sites with different σ will have a second-order lowering $\Delta E^{(2)} = -4t^2/U$. The entropy per site is lower than ln(3). Thus while mean-field theory successfully captures the zero temperature phase diagram as was verified with QMC [6] and predicts many qualitatively correct results for the finite temperature phase diagram, it cannot capture the low temperature entropy curves in the Mott region.

Next we examine the isentropes at a noncommensurate filling. Figure 4 shows the isentropic curves for $\rho = 0.7$ overlaid on the finite temperature phase diagram. As in the commensurate filling case, here we also find that the heating-cooling separatrix is on the SF-Normal phase boundary. However, the low temperature isentropes here do not terminate at the phase boundary. Since the phase boundary for noninteger fillings never touches the $T = 0$ line, the isentropes can remain under the phase boundary for arbitrary U_0.

We present isentropes for $U_2 \neq 0$ at commensurate filling $\rho = 1$ in Fig. 5, which shows the isentropic curves for both ferromagnetic and antiferromagnetic cases for two different spin couplings. We also show the SF-MI phase boundaries on the same plot. The central observations are that the isentropes here have the same general property as for $U_2 = 0$—there is cooling in the SF phase and heating in the MI phase, the phase boundary coincides with the heating-cooling separatrix, and the low entropy lines do not enter the Mott phase. For $U_2 = -0.1U_0$ and $U_2 = 0.1U_0$, the isentropes are not much different from each other and from the $U_2 = 0$ case. However, for larger magnetic coupling, $U_2 = -0.4U_0$ [Fig. 5(b)], we find that adiabatic ramping results in a slower rate of cooling and heating. Starting with the same initial temperature and ending up at the same final optical lattice depth in the MI phase, the temperature is lower for $U_2 = -0.4U_0$ than for $U_2 = -0.1U_0$. This is also true for the polar phase $U_2 = 0.4U_0$ in Fig. 5(d).

In Fig. 6, we show the slope of the isentropes dT/dU_0 (i.e., the heating rate in the Mott and SF phases) as a function of U_2. We show results for two isentropes, $S = 1.6$ and $S = 1.2$ in the MI and SF regime. We see that the heating rate in the MI regime

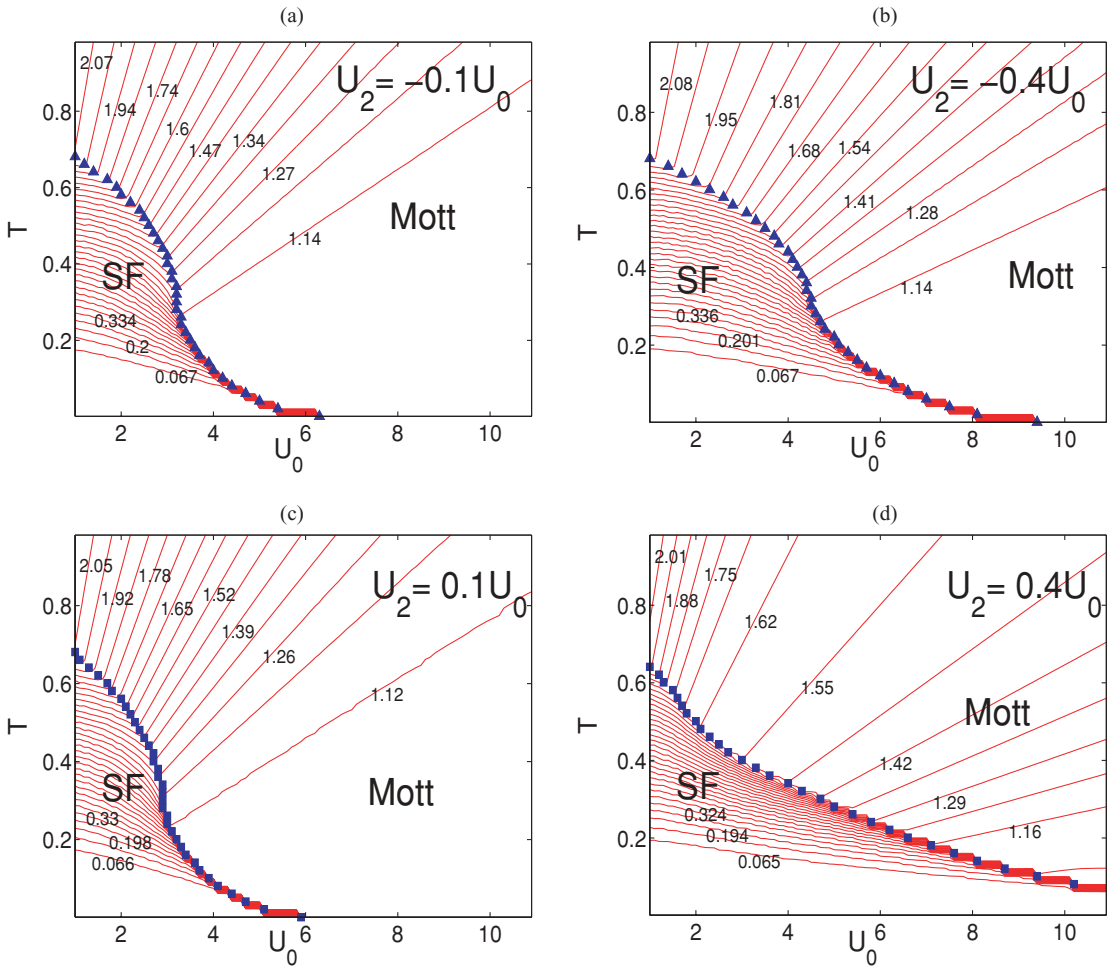

FIG. 5. (Color online) Isentropes overlaid on the finite temperature phase diagram for ferromagnetic ($U_2 < 0$) and antiferromagnetic ($U_2 > 0$) interactions. The chemical potential μ is chosen so that density $\rho = 1$. For small values of U_2, (a) $U_2 = -0.1U_0$ and (c) $U_2 = 0.1U_0$, the isentropes are not much different from each other and from $U_2 = 0$ (Fig. 3). For larger values of U_2, (b) $U_2 = -0.4U_0$ and (d) $U_2 = 0.4U_0$, the difference is more visible. Along an isentropic line, first we have cooling followed by heating for large U_0. The cooling and heating sepatrix again lies on the superfluid-Mott phase boundary.

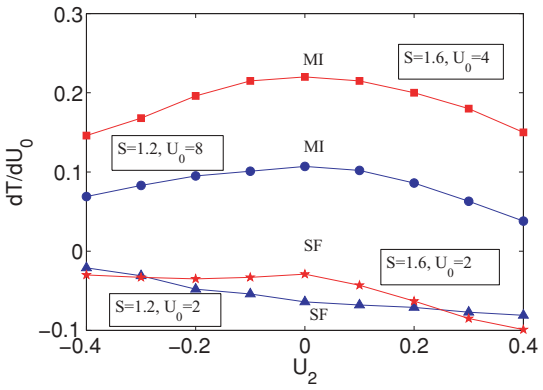

FIG. 6. (Color online) The effect of spin coupling U_2 on the rate of temperature change. As we vary U_2, the slopes of the isentropes in the (T, U_0) plane change. Here we show the rates of change of temperature with U_0 for two isentropes in the first Mott lobe and superfluid regime. In the MI region, the rate decreases as we move away from $U_2 = 0$; while in the SF, it increases or decreases depending on the value of U_0.

continually decreases as the magnitude of U_2 increases. In the SF region, the rate is negative denoting cooling. For the two isentropes we show, the characteristics of the rates differ based on whether we are in a low or higher entropy curve. For the species of atoms used in current experiments, ^{23}Na and ^{87}Rb, $|U_2|$ is on the order of 0.03. Our mean-field study indicates that the effect of magnetic couplings of this magnitude on the adiabatic heating and cooling rates is small.

From Fig. 6, we see that the rate of heating in the first Mott lobe is maximum at $U_2 = 0$, and slowly decreases as magnetic coupling is turned on for both ferromagnetic and antiferromagnetic cases. As noted earlier, increasing U_0 in the Mott region reduces fluctuations, creating order and thereby reducing entropy. Thus the system must heat as U_0 is increased to keep the entropy constant. Now if $U_2 \neq 0$, U_2 will be trying to establish another kind of order. For example, in the first Mott lobe, $U_2 > 0$ tries to establish a bond order in one dimension, and $U_2 < 0$, a ferromagnetic order. These other orders compete with the simple Mott insulator, slow down the reduction of fluctuations as U_0 is increased, and result in a slower heating rate.

In the spinless Bose-Hubbard model, the SF-MI transition in the $\rho = 1$ and $\rho = 2$ Mott lobes are qualitatively similar as they are both a second-order transition. The presence of magnetic coupling in the spin-1 model changes this scenario [7]. For $U_2 > 0$, the SF-MI transition in the $\rho = 2$ Mott lobe becomes a first-order transition. Phase boundaries for the even and odd Mott lobes also change as a function of U_2 [6,7].

Our final results address the isentropes for density $\rho = 2$. In Fig. 7 we choose $U_2 = 0$, $U_2 = -0.1U_0$, and $U_2 = 0.1U_0$. Here also we see cooling in the SF and heating in the Mott regime. Turning on the ferromagnetic coupling in Fig. 7(b) does not have a huge impact on the isentropes. However, for antiferromagnetic coupling $U_2 = 0.1U_0$ in Fig. 7(c), we see that the isentropes are visibly different as is the shape of the phase boundary. Inside the SF, the system cools down very slowly. Figure 8 shows the heating rate dT/dU_0 for a constant entropy ($S = 2.5$) in the second Mott lobe as U_2 is

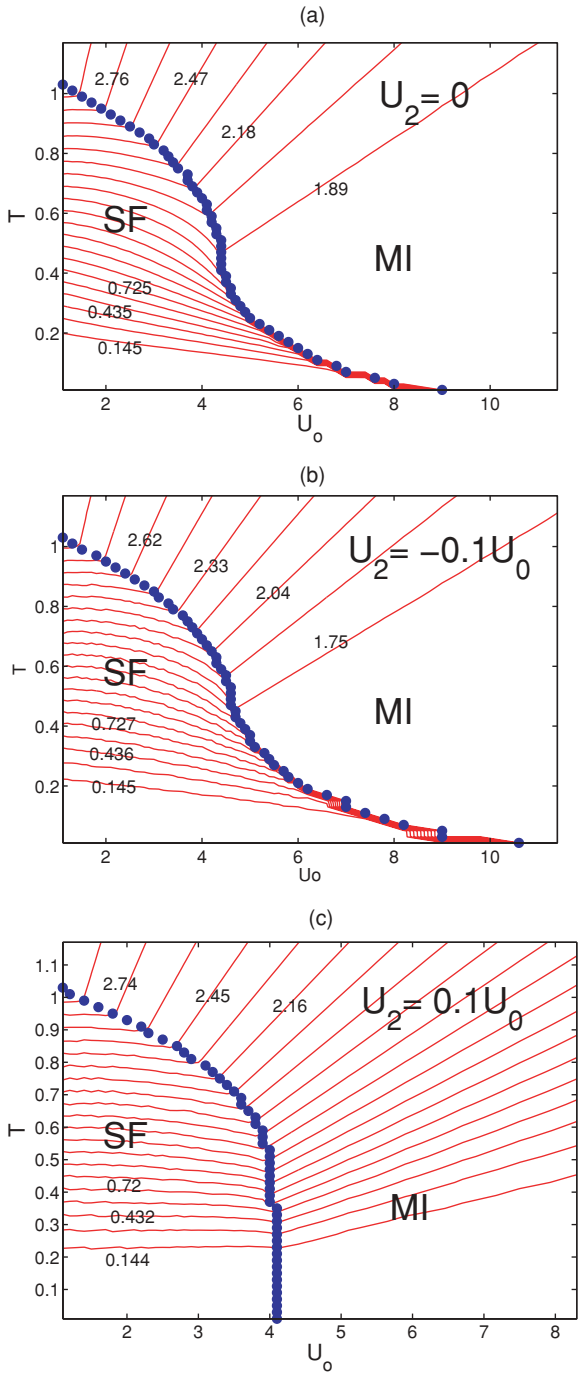

FIG. 7. (Color online) Isentropes overlaid on the finite temperature phase diagram for ferromagnetic ($U_2 < 0$) and antiferromagnetic ($U_2 > 0$) interactions for density $\rho = 2$. The same values of U_2, $U_2 = -0.1U_0$, and $U_2 = 0.1U_0$ were used as in the $\rho = 1$ results in Fig. 4. There are several differences from the case of unit filling. Here, the sign of dT/dU_0 can change within the superfluid. The isentropes no longer exhibit pure cooling. In addition, the antiferromagnetic isentropes in (c) have no terminations on the phase boundary.

turned on. Unlike the case for the first Mott lobe (Fig. 6), there is no maximum at $U_2 = 0$, and the heating rate increases monotonically with U_2. For $U_2 > 0$ and $\rho = 2$, the SF/Mott phase boundary is first order and a spin singlet phase is formed

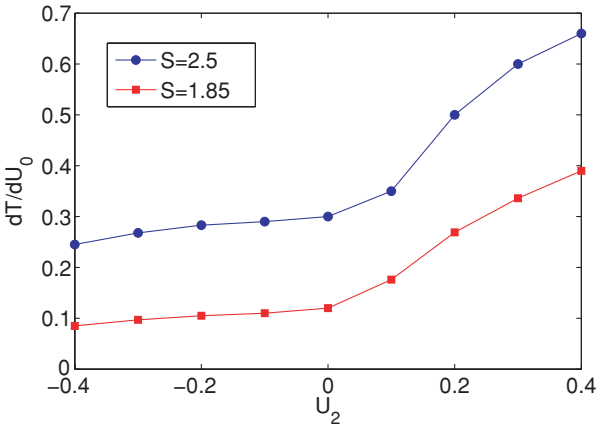

FIG. 8. (Color online) The effect of spin coupling U_2 on the rate of temperature change in the second Mott lobe ($\rho = 2$). Here we show the heating rate for two isentropes $S = 2.5$ and $S = 1.85$. Unlike the $\rho = 1$ case, the heating rate is not maximum at $U_2 = 0$, and increases for $U_2 > 0$.

in the Mott region. The appearance of order in the singlet phase greatly affects the heating properties.

IV. CONCLUSION

In this article we extended previous mean-field theory treatments of the spin-1 Bose-Hubbard model to compute the isentropic lines. These quantities are of considerable experimental importance to understand thermometry in ultracold atomic gases in an optical lattice.

We presented the isentropes in the temperature-interaction strength (T, U_0) plane for ferromagnetic, antiferromagnetic, and zero spin couplings. Following these isentropic lines, temperature changes can be determined during adiabatic loading of spin-1 bosonic atoms in an optical lattice. The isentropes have a number of interesting features. First, they exhibit pure cooling within the SF and heating in the normal or Mott phase. The phase boundary precisely corresponds to the location of the change in sign of dT/dU_0 (i.e., the heating-cooling separatrix lies on the SF-MI phase boundary). This can be understood in the symmetric view of heating as one moves away in U_0 from the phase boundary in either direction of SF/Mott. The system gets more ordered with reduced entropy. And therefore, temperature must increase to keep the entropy constant. Second, the low entropy (low temperature) isentropes terminate on the phase boundary because of the nonzero ground-state entropy, which mean-field theory gives for the Mott phase. For noncommensurate fillings, the isentropes show similar characteristics except that the low entropy lines do not terminate at the phase boundary.

The effect of ferromagnetic and antiferromagnetic couplings on isentropes was examined and we quantify the rate of heating as U_2 changes. We find that in the experimentally relevant regime of $|U_2| = 0.03$ for ^{23}Na and ^{87}Rb, the changes in heating-cooling rate is not very different from the $U_2 = 0$ case. It will be interesting to extend QMC simulations of the magnetic and superfluid properties on the spinor Bose-Hubbard model to study these thermodynamic properties as well.

ACKNOWLEDGMENTS

We thank Dave Cone and Rajiv Singh for fruitful discussions and the referee for useful observations on our calculation. This work was supported under ARO Grant No. W911NF0710576 with funds from DARPA OLE program. G.G.B. is supported by the CNRS (France) PICS 3659.

[1] M. Greiner, O. Mandel, T. Esslinger, T. W. Hänsch, and I. Bloch, Nature (London) **415**, 39 (2002).
[2] M. Leweinstein, A. Sanpera, V. Ahufinger, B. Damski, A. Sen, and U. Sen, Adv. Phys. **56**, 243 (2007).
[3] E. Demler and F. Zhou, Phys. Rev. Lett. **88**, 163001 (2002).
[4] M. Snoek and F. Zhou, Phys. Rev. B **69**, 094410 (2004).
[5] T. L. Ho, Phys. Rev. Lett. **81**, 742 (1998); S. Mukerjee, C. Xu, and J. E. Moore, *ibid.* **97**, 120406 (2006).
[6] G. G. Batrouni, V. G. Rousseau, and R. T. Scalettar, Phys. Rev. Lett. **102**, 140402 (2009).
[7] R. V. Pai, K. Sheshadri, and R. Pandit, Phys. Rev. B **77**, 014503 (2008).
[8] D. M. Stamper-Kurn, M. R. Andrews, A. P. Chikkatur, S. Inouye, H.-J. Miesner, J. Stenger, and W. Ketterle, Phys. Rev. Lett. **80**, 2027 (1998).
[9] S. Trotzky, P. Cheinet, S. Flling, M. Feld, U. Schnorrberger, A. M. Rey, A. Polkovnikov, E. A. Demler, M. D. Lukin, and I. Bloch, Science **319**, 295 (2007).
[10] Q. Zhou and T. L. Ho, e-print arXiv:0908.3015.
[11] Q. Zhou, Y. Kato, N. Kawashima, and N. Trivedi, e-print arXiv:0901.0606.
[12] R. B. Diener, Q. Zhou, H. Zhai, and T. L. Ho, Phys. Rev. Lett. **98**, 180404 (2007); W. Yi, G. D. Lin, and L. M. Duan, Phys. Rev. A **76**, 031602(R) (2007).
[13] I. B. Spielman, W. D. Phillips, and J. V. Porto, Phys. Rev. Lett. **98**, 080404 (2007).
[14] A. M. Rey, G. Pupillo, and J. V. Porto, Phys. Rev. A **73**, 023608 (2006).
[15] S. Yoshimura, S. Konabe, and T. Nikuni, Phys. Rev. A **78**, 015602 (2008).
[16] L. Pollet, C. Kollath, K. Van Houcke, and M. Troyer, New J. Phys. **10**, 065001 (2008).
[17] F. Werner, O. Parcollet, A. Georges, and S. R. Hassan, Phys. Rev. Lett. **95**, 056401 (2005).
[18] T. Paiva, R. T. Scalettar, M. Randeria, and N. Trivedi, e-print arXiv:0906.2141.
[19] V. Apaja and O. F. Syljuasen, Phys. Rev. A **74**, 035601 (2006).
[20] M. Rizzi, D. Rossini, G. DeChiara, S. Montangero, and R. Fazio, Phys. Rev. Lett. **95**, 240404 (2005); S. Bergkvist, I. P. McCulloch, and A. Rosengren, Phys. Rev. A **74**, 053419 (2006).

[21] K. Sheshadri, H. R. Krishnamurthy, R. Pandit, and T. V. Ramakrishnan, Europhys. Lett. **22**, 257 (1993).
[22] K. V. Krutitsky and R. Graham, Phys. Rev. A **70**, 063610 (2004); K. V. Krutitsky, M. Timmer, and R. Graham, *ibid.* **71**, 033623 (2005).
[23] T. Kimura, S. Tsuchiya, and S. Kurihara, Phys. Rev. Lett. **94**, 110403 (2005); S. Tsuchiya, S. Kurihara, and T. Kimura, Phys. Rev. A **70**, 043628 (2004).
[24] M. C. Chung and S.-K. Yip, e-print arXiv:0904.4110; M. C. Chung and S.-K. Yip, e-print arXiv:0811.2054.
[25] A. V. Chubukov, Phys. Rev. B **43**, 3337 (1991).
[26] A. Imambekov, M. Lukin, and E. Demler, Phys. Rev. A **68**, 063602 (2003); Phys. Rev. Lett. **93**, 120405 (2004).
[27] P.-A. Lindgard, H. E. Viertio, and O. G. Mouritsen, Phys. Rev. B **38**, 6798 (1988).
[28] D. Cone and R. T. Scalettar (unpublished).